2013 IEEE International Conference on Robotics and Automation (ICRA)
Karlsruhe, Germany, May 6-10, 2013

Microassembly using a Cluster of Paramagnetic Microparticles

Islam S. M. Khalil*, Frank van den Brink*, Ozlem Sardan Sukas† and Sarthak Misra*
University of Twente, The Netherlands

***Abstract*— We use a cluster of paramagnetic microparticles to carry out a wireless two-dimensional microassembly operation. A magnetic-based manipulation system is used to control the motion of the cluster under the influence of the applied magnetic fields. Wireless motion control of the cluster is implemented at an average velocity and maximum position tracking error of 144 μm/s and 50 μm, respectively. This control is used to achieve point-to-point positioning of the cluster, manipulation of microobjects, and assembly of microobjects into a microstructure. The control system achieves stable positioning of the cluster, while simultaneously compensating for the planar drag forces on the cluster and the microobject. The presented magnetic-based microassembly technique allows for the selective pushing and pulling of microobjects with specific geometries towards their destinations inside a microstructure in an execution time of 18 s, within a workspace of 1.8 mm $\times$ 2.4 mm.**

I. INTRODUCTION

The continuous demand for miniaturization motivated the development of new microassembly and micromanipulation techniques [1]-[8]. Some of these techniques depend on the wireless power transmission to guide and/or steer magnetic objects such as microorganisms, microrobots or microparticles. These magnetic entities can then be utilized to push and pull microobjects to accomplish microassembly operations. Microassembly using a swarm of magnetotactic bacteria was realized by Martel *et al.* [9], where a directional magnetic field was generated to control a swarm of magnetotactic bacteria by applying magnetic torque on the magnetite nanocrystals of the bacteria. A layer of motile bacteria, i.e., *Serratia marcescene*, were integrated with a microstructure, and controlled by the self-propulsion and DC electric fields using a vision feedback control system [10]. The aforementioned techniques benefit from the self-propulsion generated by the flagella bundles or cilia to provide thrust force during the manipulation of microobjects. The maximum thrust force generated by either the flagella bundle or the cilia is in the range of pico-Newton [11], [12].

In order to provide greater thrust forces than the propulsion forces of the magnetic microorganisms, we use a cluster of paramagnetic microparticles to steer and orient microobjects. Such cluster, has an oriented magnetic dipole moment *only* under an external magnetic field [13]. This magnetic dipole moment allows us to control the position and the orientation of the cluster under the influence of magnetic fields to accomplish microassembly operations, as shown in Fig. 1.

*Islam S. M. Khalil, Frank van den Brink and Sarthak Misra are with MIRA–Institute for Biomedical Technology and Technical Medicine.
†Ozlem Sardan Sukas is with MESA+ Institute for Nanotechnology.
The authors thank Leon Abelmann for the valuable feedback during preparation of this manuscript.

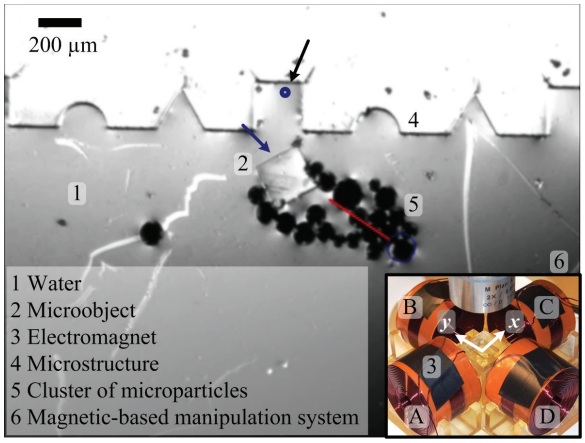

Fig. 1. Assembly of a microobject to a microstructure using a cluster of microparticles. The controlled cluster selectively positions the microobject inside a microstructure. Motion of the cluster is controlled under the influence of the external magnetic fields generated by the magnetic-based manipulation system, provided in the inset. The cluster of microparticles, microobject and microstructure are immersed in water within a reservoir. The blue (light) circle is assigned by our feature tracking software [14], whereas the small blue circle indicates a reference position. The red line represents the velocity vector of the cluster. The black and blue arrows indicate the reference position and the microobject, respectively. The letters A, B, C and D indicate the electromagnets.

This work addresses the utilization of a cluster of microparticles to accomplish a two-dimensional microassembly operation. We utilize a magnetic-based manipulation system to control the motion of the cluster [14], [15]. The relation between the number of microparticles within the cluster and its average linear velocity is experimentally analyzed. This analysis allows us to choose an optimal number of microparticles within our cluster. A closed-loop control system is then designed to allow for the point-to-point positioning of the cluster along with the simultaneous compensation of the drag forces on the cluster and the microobject. This control is used to selectively manipulate and assemble microobjects to a microstructure.

The remainder of this paper is organized as follows: In Section II we discuss the modeling and the closed-loop control of a cluster of microparticles. In Section III, we provide descriptions for our experimental setup, i.e., a magnetic-based manipulation system, and the fabrication steps of the microobjects and the microstructure utilized in the microassembly operation. Section IV provides our experimental results which includes point-to-point motion control of the cluster, micromanipulation of microobjects and

a microassembly operation. Finally, Section V concludes and provides directions for future work.

II. MODELING AND CONTROL

A cluster of microparticles experiences a resultant magnetic force and torque upon the application of a magnetic field. The magnetic force and torque must overcome the drag force and torque, respectively, during the motion of the cluster in a fluid. We control the magnetic force to execute microassembly operations using the cluster.

A. Modeling of a Cluster of Microparticles

The magnetic force experienced by a cluster of microparticles is given by

$$\mathbf{F}(\mathbf{P}) = \nabla(\mathbf{m}(\mathbf{P}) \cdot \mathbf{B}(\mathbf{P})), \tag{1}$$

where $\mathbf{F}(\mathbf{P}) \in \mathbb{R}^{3\times1}$ is the magnetic force. Further, $\mathbf{m}(\mathbf{P}) \in \mathbb{R}^{3\times1}$ and $\mathbf{B}(\mathbf{P}) \in \mathbb{R}^{3\times1}$ are the induced magnetic dipole moment of the cluster and the magnetic field at point ($\mathbf{P} \in \mathbb{R}^{3\times1}$), respectively. The cluster also experiences a magnetic torque given by

$$\mathbf{T}(\mathbf{P}) = \mathbf{m}(\mathbf{P}) \times \mathbf{B}(\mathbf{P}). \tag{2}$$

In (2), $\mathbf{T}(\mathbf{P}) \in \mathbb{R}^{3\times1}$ is the magnetic torque. The cluster moves in a fluid. Therefore, it experiences the following drag force:

$$\mathbf{F}_{\mathrm{dc}}(\dot{\mathbf{P}}) = \digamma_{\mathrm{c}}\eta\dot{\mathbf{P}}, \tag{3}$$

where $\mathbf{F}_{\mathrm{dc}}(\dot{\mathbf{P}}) \in \mathbb{R}^{3\times1}$ is the drag force on the cluster. Further, $\digamma_{\mathrm{c}}$ and η are the shape factor of the cluster and the dynamic viscosity of the fluid, respectively. The microobject also experiences a drag force given by

$$\mathbf{F}_{\mathrm{do}}(\dot{\mathbf{P}}) = \digamma_{\mathrm{o}}\eta\dot{\mathbf{P}}. \tag{4}$$

In (4), $\mathbf{F}_{\mathrm{do}}(\dot{\mathbf{P}}) \in \mathbb{R}^{3\times1}$ is the drag force on the microobject, and $\digamma_{\mathrm{o}}$ is the shape factor of the microobject. We assume that the microobject has the same velocity as the cluster. Our objective is to use the cluster to steer microobjects towards specific positions within a microstructure. Therefore, the magnetic force must overcome the drag forces experienced by both the cluster and the microobject.

B. Closed-Loop Control

The motion of the cluster is governed by the following equation of motion:

$$\mathbf{F}(\mathbf{P}) - \mathbf{F}_{\mathrm{dc}}(\dot{\mathbf{P}}) - \mathbf{F}_{\mathrm{do}}(\dot{\mathbf{P}}) = \mathrm{M}\ddot{\mathbf{P}}, \tag{5}$$

where M is the mass of the cluster. In order to allow the cluster to follow any reference position ($\mathbf{P}_{\mathrm{ref}}$) within the workspace of our magnetic-based manipulation system, we devise the following controlled magnetic force ($\mathbf{F}_{\mathrm{c}}(\mathbf{P})$):

$$\mathbf{F}_{\mathrm{c}}(\mathbf{P}) = \widehat{\mathbf{F}}_{\mathrm{d}}(\dot{\mathbf{P}}) + \mathrm{M}_{\mathrm{n}}\left(\ddot{\mathbf{P}}_{\mathrm{ref}} - \mathbf{K_d}\dot{\mathbf{e}} - \mathbf{K_p}\mathbf{e}\right). \tag{6}$$

In (6), $\mathbf{K_p}$ and $\mathbf{K_d}$ are the controller positive-definite gain matrices, and are given by

$$\mathbf{K_p} = \begin{bmatrix} k_{\mathrm{p1}} & 0 \\ 0 & k_{\mathrm{p2}} \end{bmatrix} \text{ and } \mathbf{K_d} = \begin{bmatrix} k_{\mathrm{d1}} & 0 \\ 0 & k_{\mathrm{d2}} \end{bmatrix}, \tag{7}$$

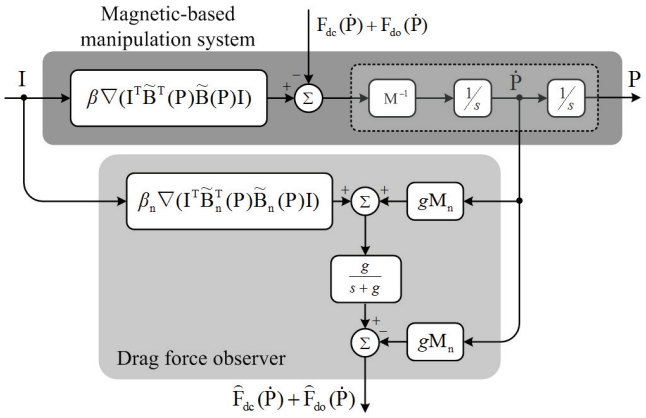

Fig. 2. Drag force observer [16]-[18]: Drag forces on the cluster of microparticles ($\mathbf{F}_{\mathrm{dc}}(\dot{\mathbf{P}})$) and microobject ($\mathbf{F}_{\mathrm{do}}(\dot{\mathbf{P}})$) are estimated using the applied current ($\mathbf{I}$) to each of the electromagnets, and the velocity ($\dot{\mathbf{P}}$) of the cluster. The estimated drag forces ($\widehat{\mathbf{F}}_{\mathrm{dc}}(\dot{\mathbf{P}})$ and $\widehat{\mathbf{F}}_{\mathrm{do}}(\dot{\mathbf{P}})$) are used by the control law (6) to compensate for the drag forces. M and M_{n} are the mass of the cluster and its nominal value, respectively. Further, g is a positive gain of the low-pass filter associated with the drag force observer. β is a magnetic constant, and β_n represents its nominal value.

where $k_{\mathrm{p}i}$ and $k_{\mathrm{d}i}$, for $(i = 1, 2)$, are the proportional and derivative gains, respectively. Further, in (6), $\widehat{\mathbf{F}}_{\mathrm{d}}(\dot{\mathbf{P}})$ is the estimated drag force, and is given by

$$\widehat{\mathbf{F}}_{\mathrm{d}}(\dot{\mathbf{P}}) \triangleq \widehat{\mathbf{F}}_{\mathrm{dc}}(\dot{\mathbf{P}}) + \widehat{\mathbf{F}}_{\mathrm{do}}(\dot{\mathbf{P}}), \tag{8}$$

where $\widehat{\mathbf{F}}_{\mathrm{dc}}(\dot{\mathbf{P}})$ and $\widehat{\mathbf{F}}_{\mathrm{do}}(\dot{\mathbf{P}})$ are the estimated drag forces on the cluster and the microobject, respectively. Moreover, M_{n} is the nominal mass of the cluster. The drag force is estimated using the following drag force observer [16]-[18]:

$$\widehat{\mathbf{F}}_{\mathrm{d}}(\mathbf{P}) = \frac{g}{s+g}\left[\mathbf{F}(\mathbf{P}) + g\mathrm{M}_{\mathrm{n}}\dot{\mathbf{P}}\right] - g\mathrm{M}_{\mathrm{n}}\dot{\mathbf{P}}. \tag{9}$$

In (9), g is a positive gain of the low-pass filter associated with the drag force observer, shown in Fig. 2. In the realization of the drag force observer (9), the magnetic force is explicitly represented by the current vector ($\mathbf{I}$) using

$$\mathbf{F}(\mathbf{P}) = \beta\nabla\left(\mathbf{I}^{\mathrm{T}}\widetilde{\mathbf{B}}^{\mathrm{T}}(\mathbf{P})\widetilde{\mathbf{B}}(\mathbf{P})\mathbf{I}\right), \tag{10}$$

where $\widetilde{\mathbf{B}}(\mathbf{P}) \in \mathbb{R}^{3\times e}$ is a matrix which depends on the position at which the magnetic field is evaluated. This matrix maps the input current onto magnetic field by [8], [19]

$$\mathbf{B}(\mathbf{P}) = \sum_{i=1}^{e}\mathbf{B}_i(\mathbf{P}) = \sum_{i=1}^{e}\widetilde{\mathbf{B}}_i(\mathbf{P})I_i = \widetilde{\mathbf{B}}(\mathbf{P})\mathbf{I}. \tag{11}$$

In (10), β is a magnetic constant, and is given by [15]

$$\beta \triangleq \frac{4n}{3}\frac{1}{\mu}\pi r_{\mathrm{p}}^3\chi_{\mathrm{m}}, \tag{12}$$

where χ_{m} and μ are the magnetic susceptibility constant and the permeability coefficient, respectively [20]. Moreover, r_{p} and n are the average radius of the spherical microparticle and the number of microparticles within the cluster, respectively. In (11), e is the number of electromagnets within our magnetic-based manipulation system. Further,

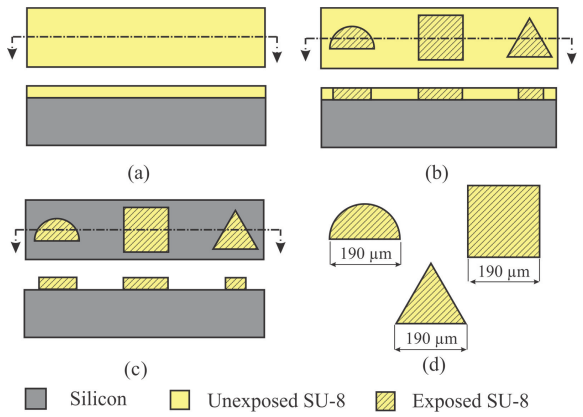

Fig. 3. Fabrication steps of the microobjects: (a) Spin coating of SU-8 (MicroChem Corp., Newton, USA) on a silicon wafer. (b) Transferring the patterns of the microobjects to the SU-8 layer after pre-bake and ultraviolet-exposure. (c) Realization of the microobjects after post-exposure bake and developing the unexposed SU-8 layer. (d) Microobjects are released by etching the silicon wafer.

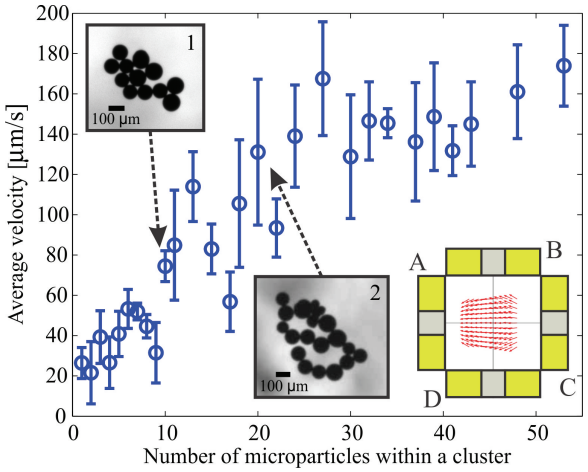

Fig. 4. Average velocity of the cluster versus the number of microparticles in the cluster. Each average velocity is calculated from 5 motion control trials. Electromagnet A (provided by the inset at bottom right corner) is used to pull the cluster by the field gradients. These gradients are generated by applying 1 A to electromagnet A. The velocity is proportional to the number of microparticles within the cluster, then the velocity approximately reaches to an asymptote at an average velocity of 140 μm/s, and 20 microparticles per cluster. Inset 1 and 2 show two clusters of 12 and 19 microparticles, respectively. Paramagnetic microparticles with average diameter of 100 μm are used in this experiment (PLAParticles-M-redF-plain from Micromod Partikeltechnologie GmbH, Rostock-Warnemuende, Germany).

$\mathbf{B}_i(\mathbf{P})$ represents the magnetic field generated by the ith electromagnet, and I_i denotes its applied current. The drag force observer estimates the drag forces on the cluster and the microobject using the nominal model of the magnetic system, the input current $(\mathbf{I})$ and velocity $(\dot{\mathbf{P}})$ of the cluster (the nominal parameters are indicated by the subscript n). The exact models of the drag forces (3) and (4) do not have to be known during the estimation of these forces using (9).

The position $(\mathbf{e})$ and velocity $(\dot{\mathbf{e}})$ tracking errors of the cluster are given by

$$\mathbf{e} = \mathbf{P} - \mathbf{P}_{\mathrm{ref}} \text{ and } \dot{\mathbf{e}} = \dot{\mathbf{P}} - \dot{\mathbf{P}}_{\mathrm{ref}}, \tag{13}$$

where $\mathbf{P}_{\mathrm{ref}}$ and $\dot{\mathbf{P}}_{\mathrm{ref}}$ are the reference position and velocity, respectively. Substitution of the controlled magnetic force (6) in (5) yields the following tracking error dynamics:

$$\ddot{\mathbf{e}} + \mathbf{K_d}\dot{\mathbf{e}} + \mathbf{K_p}\mathbf{e} = 0. \tag{14}$$

Therefore, the desired magnetic force allows the cluster to follow a reference position, while simultaneously compensating for the two-dimensional drag forces on the cluster and the microobject.

III. EXPERIMENTAL SETUP

Our experimental work is carried out on a magnetic-based manipulation system to control the motion of the cluster. We fabricate microobjects and a microstructure to investigate experimentally our magnetic-based microassembly technique.

A. Magnetic-Based Manipulation System

A cluster of paramagnetic microparticles (PLAParticles-M-redF-plain from Micromod Partikeltechnologie GmbH, Rostock-Warnemuende, Germany) with an average diameter of 100 μm is immersed inside a water reservoir. This reservoir is surrounded by an orthogonal array of four electromagnets. The array of electromagnets generates a magnetic field and gradient of the magnetic field squared in excess of 15 mT and 5 mT^2/m, respectively. Such magnetic field and gradient allow the cluster of microparticles to overcome the rotational and linear drag forces, respectively. Position of the cluster is tracked by a microscopic system and a feature tracking software. Detailed descriptions of our magnetic system are provided in [14], [21].

B. Fabrication of Microobjects and Microstructure

In order to carry out microassembly operations using our magnetic-based manipulation system, we fabricate microobjects and a microstructure using SU-8-50 and SU-8-100, respectively (MicroChem Corp., Newton, USA). A silicon wafer with <100> crystal orientation is spin coated with a layer of SU-8-50 (Fig. 3(a)). The thickness and diameter of this wafer are 500 μm and 100 μm, respectively. After, pre-baking the wafer, patterns of the microobjects are transferred to the SU-8 layer by ultraviolet (UV) exposure (Fig. 3(b)). The wafer is then post-exposure-baked and the microobjects are realized by developing the SU-8 layer in RER600 (ARCH Chemicals, Basel, Switzerland) (Fig. 3(c)). Mechanical stability of the microobjects is achieved by hard baking the wafer. Oxygen plasma treatment of the microobjects (30 s) is done to make them hydrophilic. Finally, the microobjects are released by etching the silicon wafer in a 5 wt% Tetramethylammonium hydroxide solution at 85°C (Fig. 3(d)). The aforementioned procedures are also followed during the fabrication of the microstructure, shown in Fig. 1. However, the microstructure is not released by etching the silicon wafer. Instead, the silicon wafer is diced into 11 mm^2 chip to hold the microstructure inside the reservoir of the magnetic system.

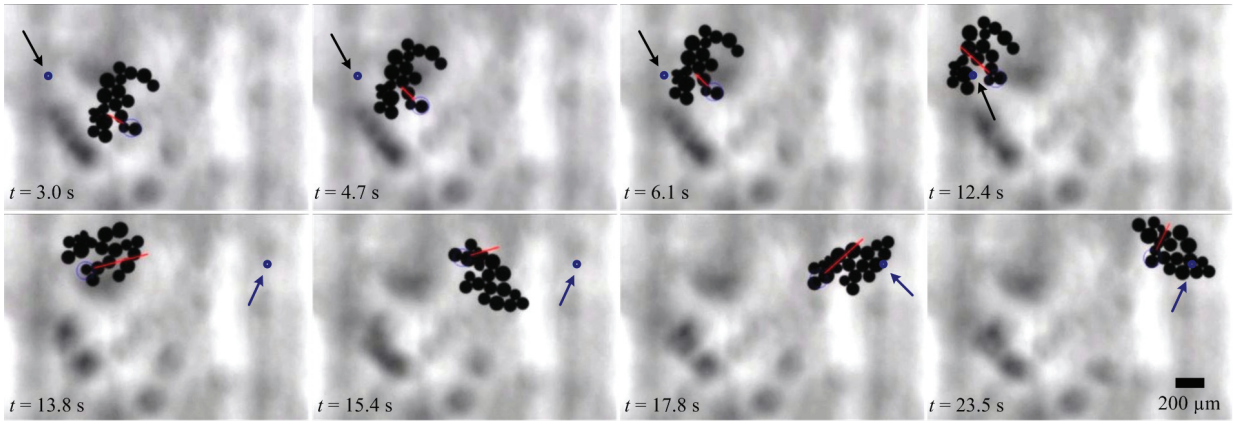

Fig. 5. Motion control of a cluster of microparticles under the influence of the applied magnetic fields at various time (t) instants. The cluster follows two reference positions indicated by the black and blue arrows in the upper and bottom rows, respectively. The cluster follows these reference positions at a velocity of 144 μm/s, and maximum position tracking error of 50 μm. This motion control experiment is done using the control law (6). The controller gains are: $k_{\mathrm{p1}} = k_{\mathrm{p2}} = 10\ \mathrm{s}^{-2}$, $k_{\mathrm{d1}} = k_{\mathrm{d2}} = 20\ \mathrm{s}^{-1}$, and $g = 30$ rad/s. The cluster consists of 19 microparticles. Paramagnetic microparticles with average diameter of 100 μm are used in this experiment (PLAParticles-M-redF-plain from Micromod Partikeltechnologie GmbH, Rostock-Warnemuende, Germany). The large blue (light) circle is assigned by our feature tracking software [14], whereas the small blue circles indicate the reference positions. The red (light) line represents the velocity vector of the cluster. *Please refer to the attached video that demonstrates the results of the point-to-point control of the cluster.*

IV. EXPERIMENTAL RESULTS

Our experimental work includes point-to-point motion control of the cluster, micromanipulation of microobjects by pushing or pulling, and microassembly of a microobject to the microstructure. In order to carry out the aforementioned experiments, we experimentally investigate the relation between the number of microparticles within the cluster and the average linear velocity of the cluster. The experimental parameters and gains of the control system utilized throughout our experimental work are provided in Table I.

A. Cluster of Microparticles

The magnetic force is linearly proportional to the volume and the number of microparticles within the cluster, as well as the gradient of the magnetic field squared (10). Increasing the volume or the number of microparticles in the cluster, to overcome the drag forces (3) and (4), limits the workspace of our magnetic system, i.e., 1.8 mm $\times$ 2.4 mm. Therefore, we analyze the effect of the number of microparticles within the cluster on its linear velocity. This analysis is done by pulling the cluster by the field gradients, and measuring the linear velocity of the cluster for different number of microparticles.

TABLE I

EXPERIMENTAL PARAMETERS AND CONTROLLER GAINS. THE CONTROLLER GAINS ARE SELECTED SUCH THAT THE MATRICES $\mathbf{K_P}$ AND $\mathbf{K_d}$ ARE POSITIVE DEFINITE.

Parameter	Value	Parameter	Value
$\max I_i$ [A]	1.0	$\max \lvert\mathbf{B}(\mathbf{P})\rvert$ [mT]	15
r_{p} [μm]	50	$\mathrm{M_n}$ [kg]	7.33×10^{-10}
n	$\sim$20	χ_{m}	0.17 ± 0.007
η [mPa.s]	1	g [rad/s]	30
$k_{\mathrm{p1,p2}}$ [s^{-2}]	10	$k_{\mathrm{d1,d2}}$ [s^{-1}]	20

We vary the number of microparticles per cluster from 1 microparticle to 55 microparticles. Each cluster is controlled five times and the average velocity is calculated, as shown in Fig. 4. The anisotropy of our workspace is considered in this experiment, and therefore all motion control trials are done along the x-axis of our magnetic system (Fig. 1). We observe that the linear velocity of the cluster increases linearly by increasing the number of microparticles, then the velocity approximately reaches to an asymptote at 140 μm/s for 20 microparticles per cluster. This analysis allows us to choose 20 microparticles per cluster, since the velocity does not increase by incorporating more particles.

B. Point-to-Point Motion Control

The control law (6) is used to realize the point-to-point motion control of the cluster of microparticles. Fig. 5 provides the motion control result of the cluster. Two reference positions are tracked at an average velocity of 144 μm/s, and with maximum position tracking error of 50 μm. This experiment demonstrates the ability of our magnetic-based manipulation system to position the cluster within our workspace. In addition, this experiment shows that the generated gradients by our magnetic system indeed overcome the drag forces on the cluster.

C. Micromanipulation of Microobjects

Micromanipulation is done by pushing and pulling the microobjects. We utilize our cluster to push the microobject towards the two reference positions provided in Fig. 6. In this experiment, a cluster of microparticles of 100 μm in diameter, is used to steer a triangular microobject with edge length of 190 μm. This experimental result demonstrates that the generated gradients overcome the drag forces on the cluster and the microobject. We observe that the average velocity and maximum position tracking error are 204 μm/s and 75 μm, respectively.

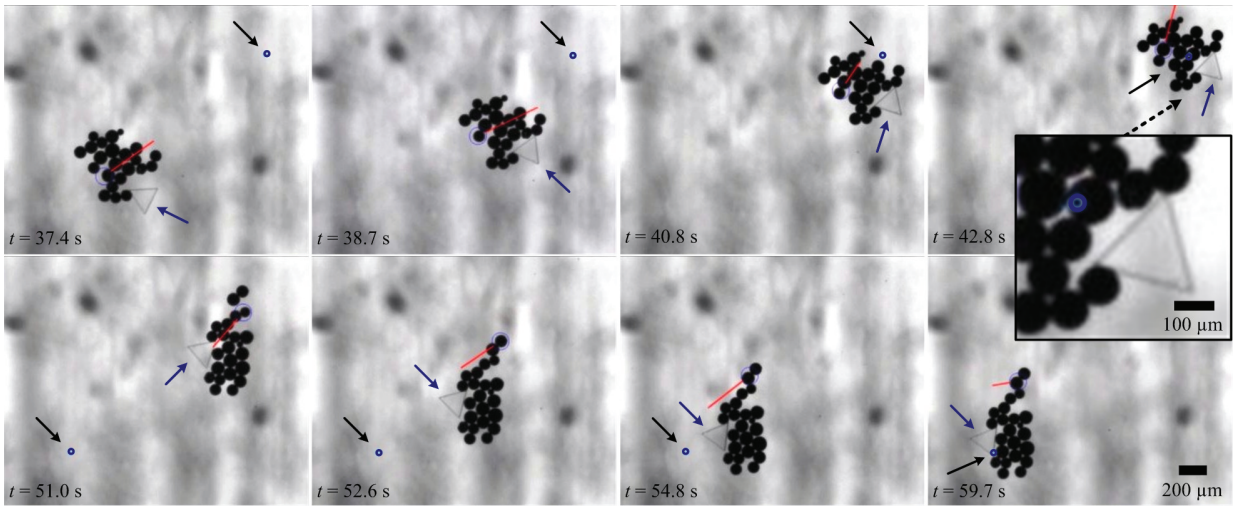

Fig. 6. Micromanipulation of a triangular microobject towards two reference positions using a cluster of microparticles at various time (t) instants. The cluster pushes the microobject under the influence of the controlled magnetic fields generated by the control law (6). In this micromanipulation experiment, the velocity of the cluster is 204 μm/s, and maximum position tracking error of 75 μm is accomplished (error between the reference position and the center of mass of the microobject). The controller gains are: $k_{\mathrm{p1}} = k_{\mathrm{p2}} = 10\ \mathrm{s}^{-2}$, $k_{\mathrm{d1}} = k_{\mathrm{d2}} = 20\ \mathrm{s}^{-1}$, and $g = 30$ rad/s. The large blue (light) circle is assigned by our feature tracking software [14], whereas the small blue circle indicates the reference position. The red (light) line represents the velocity vector of the cluster of microparticles. The black arrows indicate the first and second reference positions in the top and bottom rows, respectively. The blue arrows indicate the microobject. The cluster consists of 23 microparticles. Paramagnetic microparticles with average diameter of 100 μm are used in this experiment (PLAParticles-M-redF-plain from Micromod Partikeltechnologie GmbH, Rostock-Warnemuende, Germany). *Please refer to the attached video that demonstrates the results of the magnetic-based micromanipulation of the triangular microobject using a cluster of microparticles.*

D. Microassembly of Microstructure and Microobjects

The cluster of microparticles is used to selectively assemble a triangular microobject to a specific destination in the microstructure, as shown in Fig. 7. The triangular object has an edge length of 190 μm. Using the control law (6), the cluster positions the triangular object to its destination in 18 s. We assign fixed reference positions within the workspace of our magnetic-based manipulation system to pull and push the triangular microobject towards the correct destination of the microstructure. First, the cluster is used to pull the triangular microobject out of the rectangular destination within the microstructure (first and second frames of the top row of Fig. 7). The cluster is then used to push the triangular microobject towards the triangular destination within the microstructure (last two frames of the top row of Fig. 7). As shown in the first two frames of the bottom row of Fig. 7, the cluster pushes the microobject inside the triangular destination. The last two frames of the bottom row of Fig. 7 indicate that the cluster is moving away from the microobject after the execution of the microassembly operation. *Please refer to the attached video that demonstrates the results of the magnetic-based microassembly using a cluster of microparticles.*

V. CONCLUSIONS AND FUTURE WORK

In this paper, we investigate the feasibility of utilizing magnetic-based manipulation systems to accomplish micromanipulation and microassembly operations. A cluster of microparticles is used to manipulate and assemble microobjects to a microstructure. First, we experimentally investigate the relation between the number of microparticles and the linear velocity of the cluster. This analysis allows us to choose ~20 microparticles during the micromanipulation and the microassembly operations. Second, we devise a control system to compensate for the drag forces on the cluster and the microobjects, while achieving stable tracking error dynamics. This control system allows us to achieve point-to-point positioning of the cluster at an average velocity of 144 μm/s, and maximum position tracking error of 50 μm. In addition, the control system allows for the manipulation of microobjects at an average velocity and maximum position tracking error of 204 μm/s and 75 μm, respectively. Finally, this control system is used to selectively assemble a microobject to a microstructure. The execution time of this microassembly operation is 18 s.

Future work in the field of magnetic-based microassembly using a cluster of microparticles should include the control of the cluster in the three-dimensional space. Therefore, our magnetic-based manipulation system will be redesigned to provide auto-focusing. In addition, our magnetic system will be automated to decrease the execution time of the microassembly operations, hence increasing the efficiency of the magnetic-based microassembly technique.

REFERENCES

[1] S. Martel and M. Mohammadi, "Towards mass-scale micro-sssembly systems using magnetotactic bacteria," *International Manufacturing Science and Engineering Conference (ASME)*, vol. 2, no. 6, pp. 487-492, Oregon, USA, June 2011.

[2] S. Martel, O. Felfoul, J.-B. Mathieu, A. Chanu, S. Tamaz, M. Mohammadi, M. Mankiewicz, and N. Tabatabaei , "MRI-based medical nanorobotic platform for the control of magnetic nanoparticles and flagellated bacteria for target interventions in human capillaries," *The*

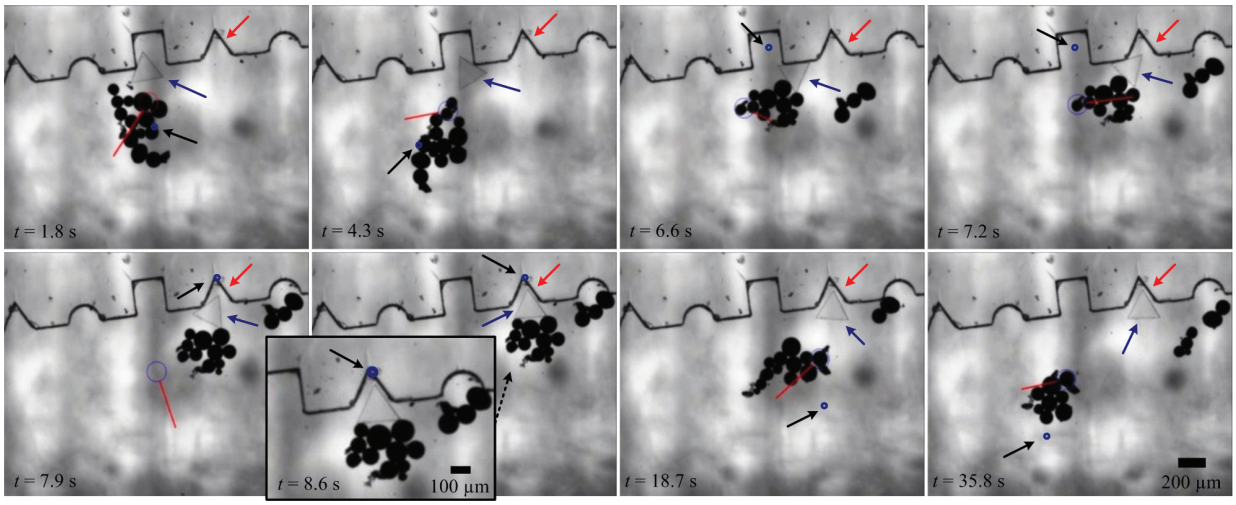

Fig. 7. Microassembly of a triangular microobject to a microstructure using a cluster of microparticles at various time (t) instants. The cluster selectively steers the microobject towards a triangular destination within the microstructure. The cluster pulls and pushes the microobject under the influence of the magnetic fields generated by the control law (6). The execution time of this microassembly operation is 18 s. In this microassembly experiment, the average velocity of the cluster is 204 μm/s, and the maximum position tracking error is 50 μm. The controller gains are: $k_{\mathrm{p1}} = k_{\mathrm{p2}} = 10\,\mathrm{s}^{-2}$, $k_{\mathrm{d1}} = k_{\mathrm{d2}} = 20\,\mathrm{s}^{-1}$, and $g = 30$ rad/s. The large blue (light) circle is assigned by our feature tracking software [14], whereas the small blue circle indicates the reference position. The red line represents the velocity vector of the cluster of microparticles. The black arrows indicate the triangular destination within the microstructure, whereas the blue arrows indicate the microobject. The microobject has an edge length of 190 μm. Paramagnetic microparticles with average diameter of 100 μm are used in this experiment (PLAParticles-M-redF-plain from Micromod Partikeltechnologie GmbH, Rostock-Warnemuende, Germany). *Please refer to the attached video that demonstrates the results of the magnetic-based microassembly using a cluster of microparticles.*

International Journal of Robotics Research, vol. 28, no. 9, pp. 1169-1182, September 2009.

[3] S. Martel, C. C. Tremblay, S. Ngakeng, and G. Langlois, "Controlled manipulation and actuation of micro-objects with magnetotactic bacteria," *Applied Physics Letters*, vol. 89, no. 23, pp. 1-3, 2006.

[4] B. J. Nelson, I. K. Kaliakatsos, and J. J. Abbott, "Microrobots for minimally invasive medicine," *The Annual Review of Biomedical Engineering*, vol. 12, pp. 55-85, April 2010.

[5] S. Floyd, C. Pawashe, and M. Sitti, "Two-dimensional contact and noncontact micromanipulation in liquid using an untethered mobile magnetic microrobot," *IEEE Transactions on Robotics*, vol. 25, no. 6, pp. 1332-1342, December 2009.

[6] C. Pawashe, S. Floyd, E. Diller, and M. Sitti, "Two-dimensional autonomous microparticle manipulation strategies for magnetic microrobots in fluidic environments," *IEEE Transactions on Robotics*, vol. 28, no. 2, pp. 467-477, April 2012.

[7] P. Valdastri, E. Sinibaldi, S. Caccavaro, G. Tortora, A. Menciassi, and P. Dario, "A Novel Magnetic Actuation System for Miniature Swimming Robots," *IEEE Transactions on Robotics*, vol. 27, no. 4, pp. 769-779, August 2011.

[8] M. P. Kummer, J. J. Abbott, B. E. Kartochvil, R. Borer, A. Sengul, and B. J. Nelson, "OctoMag: an electromagnetic system for 5-DOF wireless micromanipulation," *IEEE Transactions on Robotics*, vol. 26, no. 6, pp. 1006-1017, December 2010.

[9] S. Martel and M. Mohammadi, "Using a swarm of self-propelled natural microrobots in the form of flagellated bacteria to perform complex micro-assembly tasks," in *Proceedings of The IEEE International Conference on Robotics and Automation*, pp. 500-505, Alaska, USA, May 2010.

[10] M. S. Sakar, E. B. Steager, D. H. Kim, A. A. Julius, M. Kim, V. Kumar and G. J. Pappas, "Modeling, control and experimental characterization of microbiorobots," *The International Journal of Robotics Research*, vol. 30, no. 6, pp. 647-658, May 2011.

[11] Z. Lu and S. Martel, "Controlled bio-carriers based on magnetotactic bacteria," in *Proceedings of The IEEE International Conference on Solid-State Sensors, Actuators and Microsystems*, pp. 683-686, Lyon, France, June 2007.

[12] Z. Lu and S. Martel, "Preliminary investigation of bio-carriers using magnetotactic bacteria," in *Proceedings of The IEEE Engineering in Medicine and Biology Society Annual International Conference (EMBS)*, pp. 683-686, New York City, USA, September 2006.

[13] S. S. Shevkoplyas, A. C. Siegel, R. M. Westervelt, M. G. Prentiss, and G. M. Whitesides, "The force acting on a superparamagnetic bead due to an applied magnetic field," *Lab on a Chip*, vol. 7, no. 10, pp. 1294-1302, July 2007.

[14] J. D. Keuning, J. de Vries, L. Abelmann, and S. Misra, "Image-based magnetic control of paramagnetic microparticles in water," in *Proceedings of the IEEE International Conference of Robotics and Systems (IROS)*, pp. 421-426, San Francisco, USA, September 2011.

[15] I. S. M. Khalil, J. D. Keuning, L. Abelmann, and S. Misra, "Wireless magnetic-based control of paramagnetic microparticles," in *Proceedings of the IEEE RAS/EMBS International Conference on Biomedical Robotics and Biomechatronics (BioRob)*, pp. 460-466, Rome, Italy, June 2012.

[16] S. Komada, N. Machii, and T. Hori, "Control of redundant manipulators considering order of disturbance observer," *IEEE Transactions on Industrial Electronics*, vol. 47, no. 2, pp. 413-420, April 2000.

[17] S. Katsura, Y. Matsumoto, and K. Ohnishi, "Modeling of force sensing and validation of disturbance observer for force control," *IEEE Transactions on Industrial Electronics*, vol. 54, no. 1, pp. 530-538, February 2007.

[18] I. S. M. Khalil, R. M. P. Metz, L. Abelmann, and S. Misra, "Interaction force estimation during manipulation of microparticles," in *Proceedings of the IEEE International Conference of Robotics and Systems (IROS)*, pp. 950-956, Vilamoura, Portugal, October 2012.

[19] B. E. Kratochvil, M. P. Kummer, S. Erni, R. Borer, D. R. Frutiger, S. Schurle, and B. J. Nelson, "MiniMag: a hemispherical electromagnetic system for 5-DOF wireless micromanipulation," in *Proceedings of the 12th International Symposium on Experimental Robotics-Springer Tracts in Advanced Robotics*, New Delhi, India, December 2010.

[20] R. G. McNeil, R. C. Ritter, B. Wang, M. A. Lawson, G. T. Gillies, K. G. Wika, E. G. Quate, M. A. Howard, and M. S. Grady, "Characteristics of an improved magnetic-implant guidance system," *IEEE Transactions on Biomedical Engineering*, vol. 42, no. 8, pp. 802-808, August 1995.

[21] I. S. M. Khalil, M. P. Pichel, L. Zondervan, L. Abelmann, and S. Misra, "Characterization and control of biological microrobots," in *Proceedings of the 13th International Symposium on Experimental Robotics-Springer Tracts in Advanced Robotics*, Quebec City, Canada, June 2012.